

# Nondestructive Raman and atomic force microscopy measurement of molecular structure for individual diphenylalanine nanotubes

Banyat Lekprasert,<sup>1</sup> Victoria Sedman,<sup>2</sup> Clive J. Roberts,<sup>2</sup> Saul J. B. Tedler,<sup>2</sup> and Ioan Notingher<sup>1,\*</sup>

<sup>1</sup>*School of Physics and Astronomy, University of Nottingham, Nottingham NG7 2RD, UK*

<sup>2</sup>*School of Pharmacy, University of Nottingham, Nottingham NG7 2RD, UK*

\*Corresponding author: ioan.notingher@nottingham.ac.uk

Received October 14, 2010; revised November 11, 2010; accepted November 14, 2010;  
posted November 17, 2010 (Doc. ID 136589); published December 14, 2010

Polarized Raman microspectroscopy and atomic force microscopy were used to measure molecular orientation in individual diphenylalanine nanotubes (diameters ranging from 100 nm to 1000 nm). Analysis of the amide I Raman bands ( $1686\text{ cm}^{-1}$ ) indicated that the C=O side chains have a parallel alignment with the nanotube axis. The amide III Raman band ( $1249\text{ cm}^{-1}$ ) associated with the peptide backbone C–N vibrations showed that these bonds are preferentially aligned perpendicular to the nanotube axis. However, the Raman band corresponding to the symmetric breathing mode of the aromatic rings ( $1002\text{ cm}^{-1}$ ) indicated a rather random orientation. These results support the theoretical molecular structure models proposed recently. © 2010 Optical Society of America

OCIS codes: 300.0300, 180.5655, 170.5660.

The diphenylalanine peptide (FF), the key amyloidogenic motif of the beta-amyloid polypeptide, has recently become a focus of research interest not only because of its capacity to self-assemble, forming various nanostructures but also because of the biocompatibility and chemical versatility of the nanostructures that form [1–3]. These nanostructures have unique physical and chemical properties, such as mechanical rigidity [4] and thermal stability [5], that allow these peptide-based nanostructures to be used as potential building blocks for a variety of applications. To achieve the ultimate functionality, specifically for FF nanotubes, a thorough understanding of their physical properties as well as molecular structure is therefore important.

The proposed molecular structure of the self-assembled FF nanotubes depicts several FF molecules, NH<sub>3</sub>-Phe-Phe-COOH, arranged in a ringlike structure, where the adjacent molecules interact by head (NH<sub>3</sub><sup>+</sup>)-to-tail (-OOC) hydrogen bonds and the side-chain aromatic rings form a three-dimensional stacking [6]. However, confirmation of this theoretical model by direct experimental measurements on individual nanotubes has not been reported. Crystallographic data that were collected from experiments using x-ray diffraction techniques resulted from large specimens (needle shaped, measuring  $550\text{ }\mu\text{m} \times 266\text{ }\mu\text{m} \times 24\text{ }\mu\text{m}$ ) to maximize the diffraction intensity [7].

Measurements at single nanotube level are important because of the high heterogeneity of the FF nanotube populations. Different assembly pathways commonly lead to broad distributions in the diameter of the nanotubes, which potentially could affect their molecular structure. Many techniques with nanometer spatial resolution [atomic force microscopy (AFM), electron microscopy], which have been extensively used for studying of single FF nanotubes, have focused mainly on their physical properties (thermal stability and elasticity) [8–10]. However, these techniques lack the chemical specificity required to provide information regarding the molecular structure and orientation.

Polarized Raman spectroscopy is a noninvasive technique that can reveal molecular composition, conformation, and orientation [11] and has been applied to study many types of materials, including inorganic nanotubes and nanowires [12]. In general, two main measurement methods are used in polarized Raman experiments. The first method is performed by rotating the angle of polarization direction of the excitation laser on the investigated sample step-by-step from  $0^\circ$  to  $360^\circ$  [13,14]. To reduce the long measurement times associated with angle scanning, a second method has been reported, in which an analyzer is installed into the collection light path to enable determination of molecular orientation quantitatively from only four polarization configurations [15–17].

In our study, we used both of these polarized Raman microspectroscopy techniques to provide new insights into the molecular conformation of single FF nanotubes. A Raman microspectrometer (RMS) based on an inverted optical microscope was used to measure polarized Raman spectra with both approaches described above. An integrated AFM enabled the accurate measurement of diameters of each individual nanotube investigated.

All peptide solutions were prepared by initially solubilizing lyophilized L-diphenylalanine (FF) peptide (Genosphere, France) in 1,1,1,3,3,3-hexafluoro-2-propanol (HFIP) (Sigma Aldrich) to give a stock solution of  $100\text{ mg ml}^{-1}$ . Stock solutions were further diluted to a working concentration of  $2\text{ mg/ml}$  using ultrapure water (pH 6, resistivity  $18.2\text{ }\Omega\text{M cm}$ ). Peptide solutions were vortex mixed for 15 s to ensure complete dispersion and mixing of the sample at each stage of the preparation. Peptide solutions were allowed to equilibrate at room temperature for 24 h, and then  $50\text{ }\mu\text{l}$  aliquots were removed and deposited onto clean quartz coverslips and dried under nitrogen gas stream. Polarized Raman spectra were acquired using an in-house instrument composed of a confocal inverted Raman microscope ( $60\times$  N.A. 1.2 water immersion objective) combined with an AFM (Nanowizard II, JPK, Germany). The polarization

of the 532 nm laser was selected by a half-wave plate. A confocal pinhole (75  $\mu\text{m}$  diameter) was used to eliminate the Raman signals produced by the quartz coverslip on which the FF nanotubes were deposited. All polarized spectra were acquired using 6 mW or 12 mW laser power at three different positions on each tube with 50 s integration time (no sample deterioration was observed). In the second approach, a Glan Thomson polarizer was used as an analyzer, followed by a quarter-wave plate to eliminate the polarization dependence of the spectrometer. The  $Z$  axis was selected as the direction along the FF nanotubes. All measurements were performed under  $ZZ$ ,  $ZX$ ,  $XZ$ ,  $XX$  configurations in which the first index represents the polarization direction of the excitation laser, while the second index indicates the direction of the analyzer. The height and width of each FF nanotube diameter were measured by the integrated AFM. A total of 18 nanotubes were investigated (six for each size), and the height in the AFM images was used as a measure of nanotube diameter.

A typical AFM image showing FF nanotubes of different diameters (100 nm, 400 nm, and 600 nm) is presented in Fig. 1 along with polarized Raman spectra acquired from single FF nanotubes using the first method (no analyzer). The Raman band with strongest intensity was found at 1002  $\text{cm}^{-1}$ , which was attributed to the aromatic ring breathing mode, while other vibrations of the phenyl group are found at 1032  $\text{cm}^{-1}$ , 1190  $\text{cm}^{-1}$ , 1208  $\text{cm}^{-1}$ ,

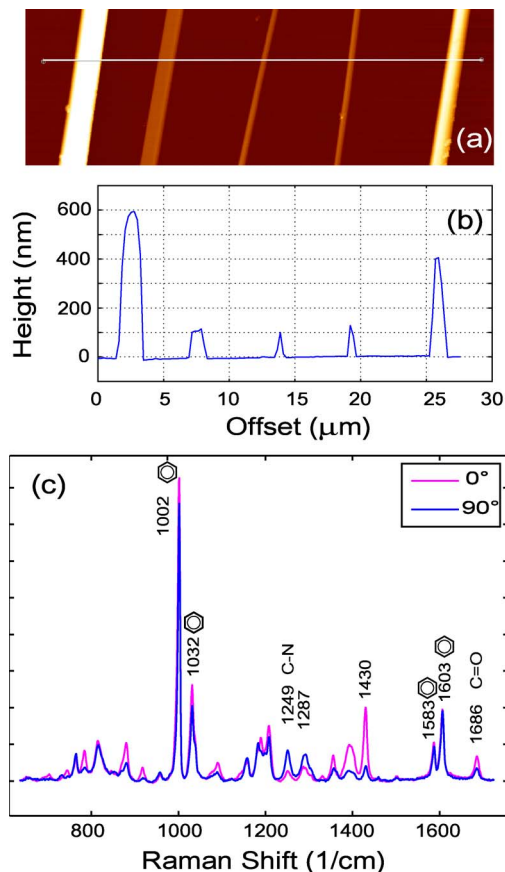


Fig. 1. (Color online) (a) Typical AFM image and (b) line profile for FF nanotubes. (c) Raman spectra of a 100 nm diameter nanotube [the middle nanotube in (a)], corresponding to 0° and 90° laser polarization relative to the nanotube axis.

1583  $\text{cm}^{-1}$ , and 1603  $\text{cm}^{-1}$  [12,14–16]. The band found at 1686  $\text{cm}^{-1}$  was assigned to the vibration of the amide I band, which corresponds mainly to the C=O stretching, while the amide III band found at 1249  $\text{cm}^{-1}$  is a highly coupled vibration, with a strong contribution from the C–N stretching [15,17–20]. The 0° spectrum was acquired when the polarization direction of the incident laser was aligned parallel to the nanotube axis, while the 90° spectrum was obtained when the polarization direction was perpendicular to the tubes. Figure 1(c) shows that several major Raman bands such as 1249  $\text{cm}^{-1}$ , 1430  $\text{cm}^{-1}$ , and 1686  $\text{cm}^{-1}$  exhibited strong dependence on the polarization directions of the excitation laser, while the bands at 1583  $\text{cm}^{-1}$  and 1603  $\text{cm}^{-1}$  were insensitive to the polarization. Therefore, these polarization-insensitive bands were used for normalization of the Raman intensity axis to enable comparison between Raman spectra of nanotubes with different diameters. In contrast, Fig. 1(c) shows that there are several Raman bands that are more intense when the laser is parallel to the tube axis (e.g., the phenyl group at 1002  $\text{cm}^{-1}$ , the amide I at 1686  $\text{cm}^{-1}$  that is assigned to the C=O), while other Raman bands are more intense for the perpendicular configuration (the amide III band at 1249  $\text{cm}^{-1}$ , which is assigned to the C–N stretching). Molecular orientation of the FF nanotubes can be described qualitatively by considering the direct plot of the selected Raman bands acquired at each polarization angle. The polar diagram in Fig. 2 shows the variation of intensity of the selected Raman bands acquired from the FF nanotubes (diameter 100 nm, 350 nm, and 900 nm) for a total rotation of 360°. The variation of the Raman bands shows that the C=O bonds are oriented parallel to the nanotube axis, while the C–N bonds are oriented perpendicular to it. The selected bands from different nanotube sizes exhibited the same orientation, which implies that they possess similar molecular orientation. The aromatic rings exhibited small variation, indicating that the phenyl groups are oriented randomly but with a slight tendency to align parallel to the tube's axis. However, this slight alignment was observed only for smaller diameter nanotubes (less than 400 nm). A more detailed description of the molecular orientation can be derived when the polarization of the scattered Raman radiation is observed. Figure 3

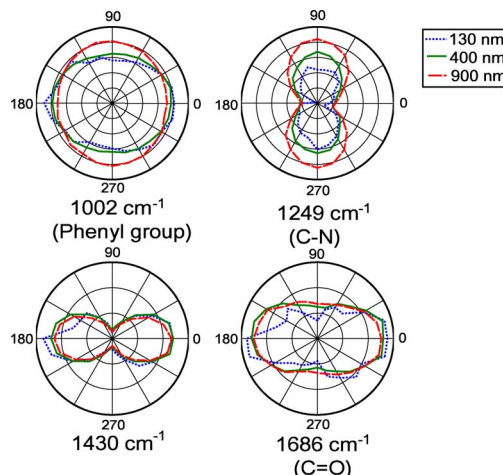


Fig. 2. (Color online) Polar diagrams for selected Raman bands.

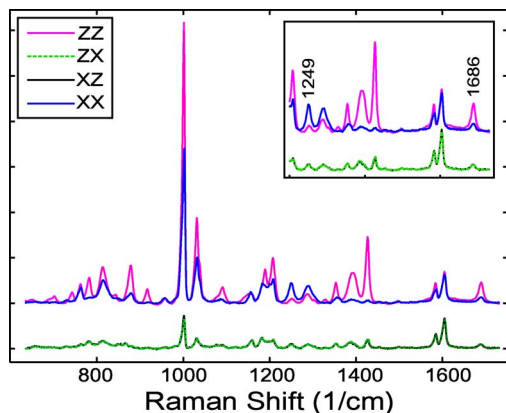


Fig. 3. (Color online) Polarized Raman spectra using the analyzer. The inset shows the enlarged spectra for the region 1200–1700  $\text{cm}^{-1}$ .

illustrates averaged polarized Raman spectra, *ZZ*, *ZX*, *XZ*, and *XX*, which were obtained from the FF nanotubes ranging between 300–400 nm in diameter. All spectra were normalized using the 1603  $\text{cm}^{-1}$  Raman band. Almost perfect overlapping between the crossed configuration, *ZX* and *XZ*, suggests that the FF nanotubes possess a fiber symmetry, which means that the molecular vibrations are independent to any rotation around the FF tube's axis. The main interest, therefore, is focused on the alignment of FF dipeptide molecules along or across the axis of the nanotube.

In the *ZZ* and *XX* spectra, the 1002  $\text{cm}^{-1}$  (phenyl group) and the 1686  $\text{cm}^{-1}$  (C=O) band exhibited stronger intensity in *ZZ* than in *XX*, while the Raman band at 1249  $\text{cm}^{-1}$  (C–N) exhibited maximum intensity in the crossed configuration *XX*. These results confirm that the C–N bond, the backbone structure of the FF molecule, is predominantly aligned across the FF tube while the side chain C=O, and that the aromatic rings are preferentially aligned along the tubes. However, the relative intensity of the 1002  $\text{cm}^{-1}$  in the polarized *ZZ* and *XX* Raman spectra changes significantly at different positions of the tube, suggesting that the orientation of the aromatic ring side chains can vary even within an individual FF nanotube.

The experimental results obtained in the polarized Raman spectra of individual FF nanotubes support the theoretical data proposed recently [6,7]. The ringlike structure due to the head ( $\text{NH}_3^+$ )-to-tail ( $-\text{OOC}$ ) hydrogen bonding polarizes the C–N vibration normal to the nanotube axis, which enhances the intensity of the Raman band (1249  $\text{cm}^{-1}$ ) in the *XX* configuration. The

C=O bonds are perpendicular on the C–N bond and are aligned along the nanotube axis, producing stronger Raman bands in the *ZZ* configuration. The FF nanotubes are formed by interactions between aromatic ring side chains, which are normal to the rings but have a rather random orientation.

This study demonstrates the potential of the combined polarized RMS-AFM technique to advance the understanding of peptide nanotube formation as well as the effect of molecular structure on their unique physical and chemical properties. Such studies could be expanded to other nanostructures, such as amyloidlike fibrils, tubular proteins, or virus shaft proteins. In addition, the AFM could also be used to induce mechanical or thermal stimulation to nanostructures, and the effects on the molecular orientation could be directly monitored by the integrated polarized RMS.

## References

1. X. Yan, P. Zhu, and J. Li, *Chem. Soc. Rev.* **39**, 1877 (2010).
2. L. Adler-Abramovich, D. Aronov, P. Beker, M. Yevnin, S. Stempler, L. Buzhansky, G. Rosenman, and E. Gazit, *Nature Nanotechnol.* **4**, 849 (2009).
3. C. H. Görbitz, *Chem. Eur. J.* **13**, 1022 (2007).
4. N. Kol, L. Adler-Abramovich, D. Barlam, R. Z. Shneck, E. Gazit, and I. Rouso, *Nano Lett.* **5**, 1343 (2005).
5. L. Adler-Abramovich, M. Reches, V. L. Sedman, S. Allen, S. J. B. Tendler, and E. Gazit, *Langmuir* **22**, 1313 (2006).
6. C. H. Görbitz, *Chem. Commun.* 2332 (2006).
7. C. H. Görbitz, *Chem. Eur. J.* **7**, 5153 (2001).
8. V. L. Sedman, S. Allen, X. Chen, C. J. Roberts, and S. J. B. Tendler, *Langmuir* **25**, 7256 (2009).
9. L. Niu, X. Chen, S. Allen, and S. J. B. Tendler, *Langmuir* **23**, 7443 (2007).
10. M. Yemini, M. Reches, J. Rishpon, and E. Gazit, *Nano Lett.* **5**, 183 (2005).
11. C. Sourisseau, *Chem. Rev.* **104**, 3851 (2004).
12. F. Lagugné-Labarthe, *Ann. Rep. Prog. Chem. C* **103**, 326 (2007).
13. G. S. Duesberg, I. Loa, M. Burghard, K. Syassen, and S. Roth, *Phys. Rev. Lett.* **85**, 5436 (2000).
14. M. Janko, P. Davydovskaya, M. Bauer, A. Zink, and R. W. Stark, *Opt. Lett.* **35**, 2765 (2010).
15. M. Rousseau, *Biomacromolecules* **5**, 2247 (2004).
16. T. Liu and S. Kumar, *Chem. Phys. Lett.* **378**, 257 (2003).
17. G. Falgayrac, S. Facq, G. Leroy, B. Cortet, and G. Penel, *Appl. Spectrosc.* **64**, 775 (2010).
18. G. Singh, A. M. Bittner, S. Loscher, N. Malinowski, and K. Kern, *Adv. Mater.* **20**, 2332 (2008).
19. B. Ravikumar, *J. Raman Spectrosc.* **37**, 597 (2006).
20. R. B. Jeffers and J. B. Cooper, *Spectrosc. Lett.* **43**, 220 (2010).